A New Experimental Method to Determine the Mutual Orientation of Helices in Coiled-Coil Proteins: Structural Information about the Dimeric Interface of cJun, cFos, GCN4, and gp41**

Wieslaw M. Kazmierski,* John McDermed, and Ann Aulabaugh

Abstract: Disruption of protein dimers interacting by a leucine zipper motif represents a new potential pharmaceutical target. However, structural information concerning the exact nature of the interacting helices is usually not available. Towards this end, we have developed a disulfide-trapping approach capable of distinguishing between the **ad** and **gd** modes of dimerization (Fig. 1), thus providing information useful in the design of small molecules that interfere with helix–helix interactions. We designed and synthesized nine cysteine-substituted peptide fragments: GCN4(**g**), GCN4(**a**), GCN4(**d**), cFos(**g**), cFos(**a**), cFos(**d**), cJun(**g**), cJun(**a**), and cJun(**d**), and evaluated the covalent crosslinking rates for them and their binary mixtures. Neither homogeneous cJun nor cFos dimerized and crosslinked, but their binary mixtures did with $t_{1/2}$ of formation **a** > **d** > **g**, indicating cFos–cJun heterodimerization according to **ad** mode (Fig. 1a). Similarly, GCN4 dimerized and crosslinked in the **ad** fashion; this result was in excellent agreement with the published X-ray structure. Next, we investigated the mode of gp41 dimerization, which appears critical for HIV-1 replication. The gp41 cysteine-substituted fragments gp41(**g**), gp41(**a**), and gp41(**d**) also dimerized and crosslinked, but with a different order of $t_{1/2}$ of formation **g** > **d** > **a**, thus providing evidence that gp41 dimerizes in the **gd** mode (Fig. 1b). Thus, the crosslinking experiments allow rapid elucidation of structural details of macromolecular interactions in aqueous media. These findings should prove useful in the design of compounds that inhibit macromolecular association.

Keywords
helices · proteins · structure elucidation · viral proteins

Introduction

Recent years have witnessed a surge of new and complex molecular targets of biomedical research. Recombinant DNA techniques have permitted the synthesis of many proteins and led to the development of several recombinant therapies based on proteins such as insulin, erythropoietin, and interleukins. The serious drawbacks of these genetically engineered drugs were soon recognized: poor oral activity, immunogenicity, and poor membrane penetration. In principle, these problems could be solved with small-molecule biomimetics designed from X-ray or NMR-derived structures of biomolecules. This paper describes a fast and robust method of generating tertiary structural information about proteins, which can then be applied to the design and synthesis of peptide mimetics. We describe a novel covalent trapping method, which will provide information about the mutual orientation of helices in coiled-coil proteins.

The α-helical motif is often involved in the process of biorecognition. Thus, interleukins 2, 4, and 7 share the same receptor subunit, which consists of alpha, beta, and gamma chains.[1] Similarly, human growth hormone interacts with its receptor through the α-helical surface.[2] A particular case involving α-helical recognition is the formation of protein dimers by coiled coils, which is often mediated by leucine zippers.[3] This motif is present in some important viral and cellular proteins such as HIV-1 integrase,[4] HIV-1 reverse transcriptase,[5] topoisomerase,[6] HSV-1 ribonucleotide reductase,[7] Epstein-Barr viral transactivator (ZEBRA),[8] and β-adrenergic receptor kinase (βARK).[9]

Another important case where formation of coiled coils seems imperative for viral proliferation is the dimeric coat protein of HIV-1, gp41.[10] A recent paper describes peptides derived from the putative coiled-coil fragment of gp41 that are able to inhibit HIV-1 replication in cell cultures. While gp41(553–590) forms highly α-helical species (by circular dichroism) in addition to dimers, formation of higher-order tetramers could not be excluded by sedimentation equilibration.[11] This result for a short peptide parallels result obtained for intact gp41, which is generally thought to be a dimer, although under specific conditions formation of its tetramers has also been detected.[10]

A recently disclosed highly constrained peptide lead, RP71955, displays a modest sequence homology to gp41(592–612) (numbering from ref. [16a]) and appears to interfere with protein assembly within gp41 itself, or between gp41 and gp120 but not between gp120 and CD4.[12]

Our goal has been to identify nonpeptide scaffolds that can mimic α-helical proteins for the purpose of disrupting protein

[*] Dr. W. M. Kazmierski, Dr. J. McDermed
Department of Medicinal Chemistry I, Glaxo Wellcome
3030 Cornwallis Rd., Research Triangle Park, NC 27709 (USA)
Fax: Int. code +(919)315-0430
Dr. A. Aulabaugh
Division of Virology, Glaxo Wellcome
Research Triangle Park, NC 27709 (USA)

[**] Part of this paper was presented at the 13th American Peptide Symposium, Edmonton, Alberta (Canada), June 20–25, 1993.

  0947-6539/96/0204-0403 $ 15.00+.25/0

dimers (multimers) of pharmaceutical interest, such as gp41. The widely accepted leucine zipper structure proposed by Landschultz[13] involves helical dimerization mediated by key amino acids on **a** and **d** positions of the helix[14] (Fig. 1). Analysis of many leucine zipper proteins suggested that the **ad** mode of dimerization may not be a general phenomenon and that other combinations are permissible. Indeed, molecular mechanics computations of the dimer stability of the fragment of GCN4, a canonical leucine zipper transcription factor, suggest that the **gd** dimer is more stable than the **ad** dimer.[15]

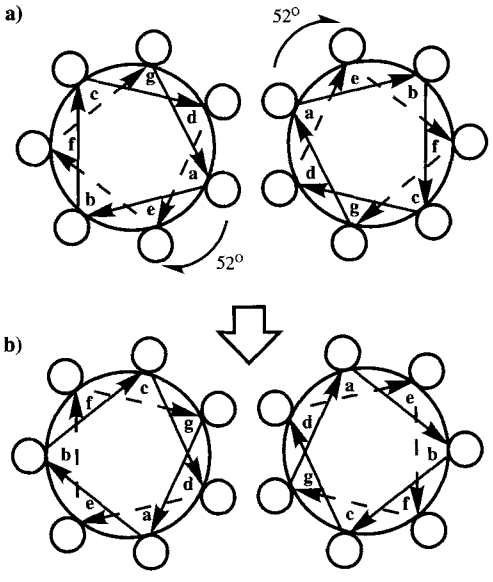

Fig. 1. A helical wheel representation of the peptide dimer: a) **a** and **d** amino acids are utilized for the dimerization; b) an alternative **gd** dimerization mode is obtained from the **ad** mode by clockwise rotation of both helices around their symmetry axes.

Because 3D structures of gp41 and of its dimer are not available, we devised a method to obtain macroscopic information about the spatial relationship of the interacting helices presumed to be involved in dimerization.[11, 16] This paper describes this method and its application to three well-known proteins: cJun, cFos, and GCN4. We also report our use of this method to postulate the dimerization mode of gp41. Our approach involved the substitution of cysteine for single amino acids in model peptides derived from the putative leucine zipper fragment of gp41. We then allowed the peptides to associate and covalently crosslink, this being possible only if both cysteines were in register. For example, in an **ad** model of dimerization (Fig. 1), placement of Cys on positions **c**, **f**, or **b** will prevent formation of the covalent dimer even if the peptides associate noncovalently. On the other hand, placement of cysteine on either position **d** or **a** in the **ad** model, or on **g** or **d** in the **gd** model, should result in efficient crosslinking. Indeed, while position **d** is nondiagnostic, **a** and **g** are diagnostic, and cysteines on these positions will or will not take part in crosslinking, depending on which mode is utilized by the dimerizing proteins.

Results

We first investigated crosslinking of Cys-substituted GCN4 fragments, GCN4(**g**): Ac-[Cys^{249}]-GCN4(249–281)-NH_2, GCN4(**a**): Ac-[Cys^{250}]-GCN4(249–281)-NH_2, and GCN4(**d**): Ac-[Cys^{253}]-GCN4(249–281)-NH_2. GCN4(**g**) eluted at 10.41 minutes on C_{18} RP HPLC (peak 2, Fig. 2a), and the covalent dimer (peak 1) formed with $t_{1/2} > 78$ h. In contrast, GCN4(**a**) formed a covalent dimer [GCN4(**a**)+GCN4(**a**)] (peak 1, Fig. 2b) rapidly ($t_{1/2} = 4$ h), and in fact within <20 h the noncovalent form (peak 2, Fig. 2b) was practically used up. Thus, cysteines in both chains of the parallel noncovalent dimer appeared positionally matched. The GCN4(**d**) peptide crosslinked with an intermediate rate ($t_{1/2}$ ca. 27 h, Fig. 2c). Comparison of the results summarized in Figures 2a–c suggests that the GCN4 dimerized according to the rules depicted in Figure 1a, which require the two hydrophobic positions **a** and **d** at the interface.

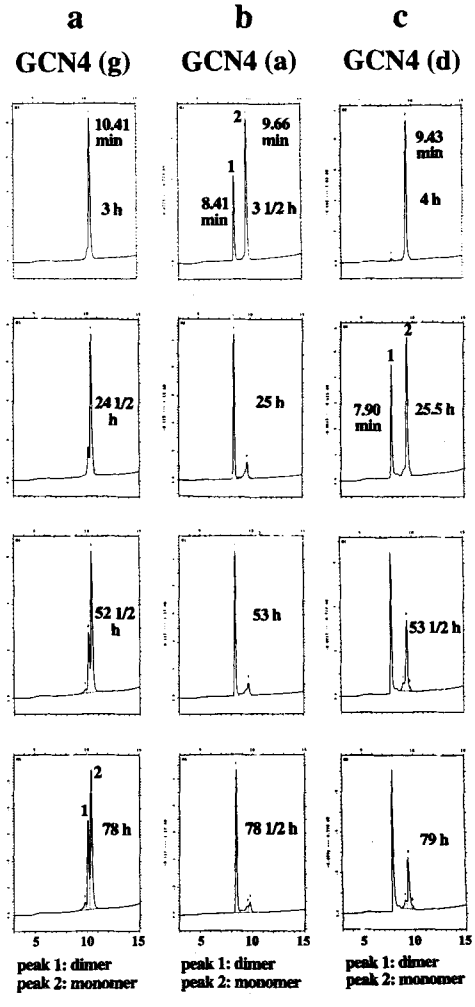

Fig. 2. HPLC traces of Ac-[Cys^x]-GCN4(249–281)-NH_2 under conditions I. a) Cys^{249} (position **g**); b) Cys^{250} (position **a**); c) Cys^{253} (position **d**).

We next investigated crosslinking of Cys-substituted cJun fragments cJun(**g**): Ac-[Cys^{276}]-cJun(276–310)-NH_2, cJun(**a**): Ac-[Cys^{277}]-cJun(276–310)-NH_2, and cJun(**d**): Ac-[Cys^{280}]-cJun(276–310)-NH_2. Peptide cJun(**g**) eluted at 9.92 min on C_{18} RP HPLC and did not form any discernible amount of covalent dimer after up to 75 h in an aqueous solution (figure not shown). The two remaining peptides, cJun(**a**) and cJun(**d**), also did not crosslink over the experiment time of >75 h (figures not shown). This result is in good agreement with the known inability of the Jun protein to dimerize at or above room temperature.[17]

We investigated crosslinking of Cys-substituted cFos fragments cFos(**g**): Ac-[Cys^{161}]-cFos(161–195)-NH_2, cFos(**a**): Ac-[Cys^{162}]-cFos(161–195)-NH_2, and cFos(**d**): Ac-[Cys^{165}]-

0947-6539/96/0204-0404 $ 15.00+.25/0 Chem. Eur. J. 1996, 2, No. 4

cFos(161–195)-NH_2. As we observed with the cJun peptides, the cFos fragments showed no tendency to dimerize (figures not shown); this is consistent with the previously observed low tendency of the cFos protein to dimerize.[17]

As an additional test of our method, we investigated possible crosslinking in heterogeneous mixtures involving all the binary combinations of GCN4(**g**), GCN4(**a**), GCN4(**d**), cJun(**g**), cJun(**a**), cJun(**d**), cFos(**g**), cFos(**a**), and cFos(**d**). Mixtures of peptides are indicated by names of both components joined with a +sign, for example, cJun(**g**)+cFos(**g**). In cases where a covalent dimer forms, a square bracket surrounds the name, for example, [cJun(**g**)+cFos(**g**)]. In the first such combination, GCN4(**g**)+GCN4(**d**) and GCN4(**a**)+GCN4(**d**) (figures not shown), formation of GCN4(**a**) dimer dominated over any other products, and neither [GCN4(**a**)+GCN4(**d**)] nor [GCN4(**g**)+GCN4(**d**)] were detected. On the other hand, in the mixture GCN4(**g**)+GCN4(**a**), about equal amounts of the homodimer [GCN4(**a**)+GCN4(**a**)] and heterodimer [GCN4(**g**)+GCN4(**a**)] were formed (not shown, but see the Experimental Section for the structural evidence for [GCN4(**g**)+GCN4(**a**)]), both allowed by the **ad** model of dimerization (Fig. 1a).

The second set of combinations, cJun(**g**)+cJun(**a**), cJun(**g**)+cJun(**d**), and cJun(**a**)+cJun(**d**), displayed no crosslinking (figures not shown). This supports previous conclusions reached in studies of homogeneous cJun peptide fragments regarding their inability to crosslink. In addition, this result indicates that the crosslinking reported here is highly sequence-specific; if it were not, scattering cysteines around the α-helical axis (**g**, **a**, **d**) would produce some background noise (nonspecific crosslinking) as a result of random collisions of the α-helical chains.

In the cFos series, peptides cFos(**g**) and cFos(**d**) exhibited similar HPLC retention times, thus obscuring the analysis. By analogy to relationships observed between the retention times for GCN4 monomer and those for GCN4 dimer (Fig. 2b), one would expect the putative cFos dimer to be more hydrophilic and thus to elute earlier from the HPLC column. Its absence suggests that pairs cFos(**g**)+cFos(**a**) and cFos(**g**)+cFos(**d**) do not produce any crosslinking products (Fig. 3a, 3b). Perhaps surprisingly, the mixture cFos(**a**)+cFos(**d**) produces a clean heterodimer product (Fig. 3c) as determined by mass spectrometry. This result is in contrast to our observations concerning homogeneous cFos fragments, in which no crosslinking was detected, as well as to some previous studies, which failed to identify the dimeric Fos.[18] However, in agreement with our result, Kim et al. also observed the dimerization and crosslinking of cysteine-substituted Fos peptide fragments,[19] with the difference that in their design cysteine was part of a flexible CGG linker, and not an intrinsic part of the α-helix, as in our peptides. The different outcome probably stems from the different concentration range (10^{-6} M) in which our dimerization studies were carried out compared with the in vitro method, which rarely yields protein concentrations higher than nanomolar. The dissociation constant for dimerization of Fos-p1 was estimated at 6 μM,[19] and so at our range of 10^{-6} M cFos can dimerize. In the [cFos(**a**)+cFos(**d**)] dimer, both sulfhydryl groups face each other in the **ad** (Fig. 1a), but not **gd** (Fig. 1b) configuration, suggesting that cFos dimerizes in an **ad** fashion.

We next explored the crosslinking preferences of heterogeneous mixtures of GCN4, cJun, and cFos peptide fragments. The trends observed in cJun and cFos cysteine-substituted peptide combinations generally matched those observed earlier. Both monomers in cJun(**g**)+cFos(**g**) (Fig. 4a) eluted with similar retention times. While the individual components cJun(**g**) and cFos(**g**) did not crosslink, the heterogeneous mixture produced a [cJun(**g**)+cFos(**g**)] covalent dimer with $t_{1/2} > 85.5$ h. The same was observed for cJun(**a**)+cFos(**a**), with the $t_{1/2}$ of formation of the covalent dimer [cJun(**a**)+cFos(**a**)] (peak 1, Fig. 4b) < 30.5 h. The cJun(**d**)+cFos(**d**) mixture again produced the covalent dimer [cJun(**d**)+cFos(**d**)] (peak 1, Fig. 4c) with $t_{1/2} = 33.5$ h.

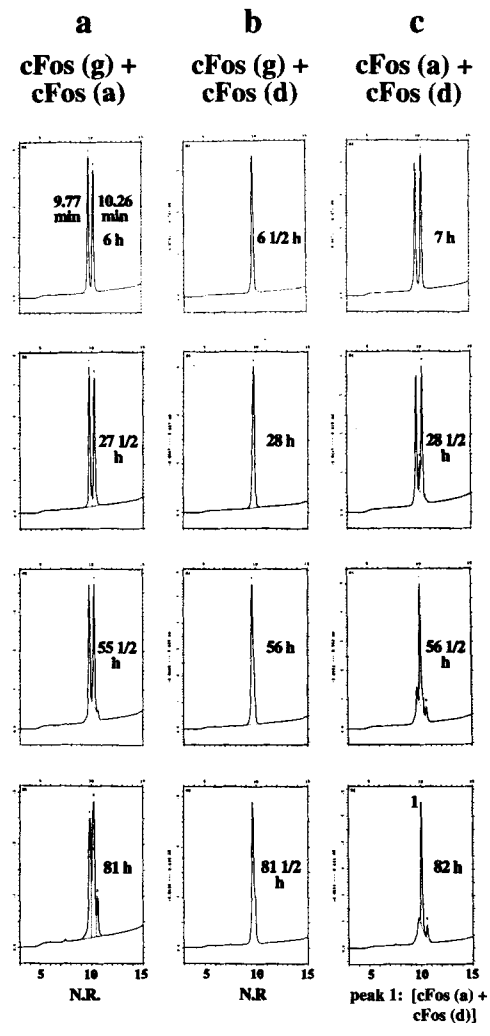

Fig. 3. HPLC traces (conditions I) of binary mixtures of Ac-[Cys^x]-cFos(161–195)-NH_2. a) Cys^{161} and Cys^{162}; b) Cys^{161} and Cys^{165}; c) Cys^{162} and Cys^{165}.

We draw two important conclusions from these results. While individual homogeneous cJun and cFos fragments do not dimerize at or above room temperature, their heterogeneous mixtures do. This is in agreement with the published experimental data[17] and it supports our assertion that the abridged peptides Ac-GCN4(249–281)-NH_2, Ac-cJun(276–310)-NH_2, and Ac-cFos(161–195)-NH_2 are adequate models of dimerization of the coiled-coil transcription factor proteins. In addition, we observed similar crosslinking rates ($t_{1/2}$ formation) among cysteine-substituted GCN4 and cJun/cFos mixtures [$t_{1/2}$(**a**) $< t_{1/2}$(**d**) $< t_{1/2}$(**g**)], again suggesting that both chains of cJun and cFos interact through hydrophobic interactions between **a** and **d** (Fig. 1a) and not mixed ionic-hydrophobic forces between **g** and **d** (Fig. 1b), as suggested by the computations.[15]

We next explored the interaction between pairs of cysteine-substituted cJun and GCN4 peptides. The pair cJun(**g**)+GCN4(**g**) did not crosslink; we only observed the (slow) ho-

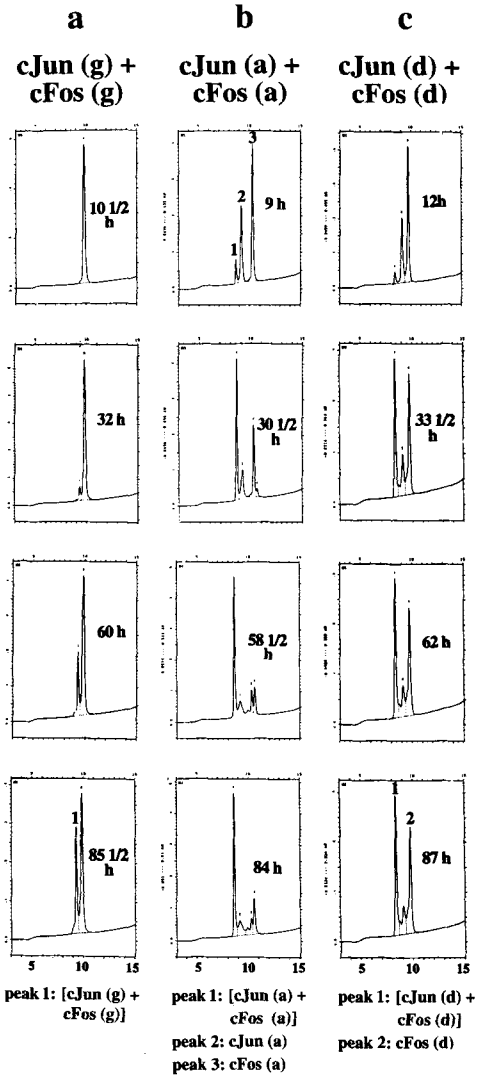

Fig. 4. HPLC traces (conditions I) of Ac-[Cys^x]-cJun(276–310)-NH_2 and Ac-[Cys^y]-cFos(161–195)-NH_2. a) $x = 276, y = 161$; b) $x = 277, y = 162$; c) $x = 280, y = 165$.

modimerization of GCN4(**g**) (figure not shown), as previously observed for pure GCN4(**g**) (Fig. 2a). In a mixture of cJun(**a**)+GCN4(**a**) (figure not shown), the GCN4(**a**) component dimerized very fast to [GCN4(**a**)+GCN4(**a**)], and no heterodimer was observed. Similarly, in cJun(**d**)+GCN4(**d**) (not shown), the GCN4 component homodimerized and crosslinked much more rapidly and, indeed, no heterodimer was formed.

Finally, similar experiments with a cFos and GCN4 binary mixture gave somewhat different results. First, cFos(**g**) +GCN4(**g**) did not form the heterodimer (not shown), while GCN4(**d**)+cFos(**d**) did (not shown), resulting in [GCN4(**d**) +cFos(**d**)] (see the Experimental Section for structural evidence) with $t_{1/2}$ approximately equal to 40 h. A mixture of cFos(**a**)+GCN4(**a**) resulted in swift formation of the [GCN4(**a**)+GCN4(**a**)] homodimer, and so the heterodimer [cFos(**a**)+GCN4(**a**)] did not form (not shown). We concluded that cFos and GCN4 can form a heterodimer, but since cysteine on position **d** is not diagnostic, we were not able to distinguish between the possible modes of interaction.

Dimerization of HIV-1 gp41: The coiled-coil gp41(555–590) is rich in hydrophobic residues, and so it is difficult to fit it a priori into a classical nomenclature of a leucine zipper. We have made a tentative alignment of its sequence with the heptad (Table 1) for purely conventional purposes and for the sake of discussion. To examine the mode of dimerization in gp41, we synthesized three model peptide fragments (numbering scheme according

Table 1. Sequences of native and cysteine-substituted GCN4, c-Jun, c-Fos and gp41 fragments used in this study.

	GCN4(249-281)	
Ac-	R M K Q L E D K V E E L L S K N Y H L E N E V A R L K K L V G E R *NH2*	
Ac-	C " " "	GCN4(g)
Ac-	R C " " "	GCN4(a)
Ac-	R M K Q C " " "	GCN4(d)
	cJUN (276-310)	
Ac-	R I A R L E E K V K T L K A Q N S E L A S T A N M L T E Q V A Q L K Q *NH2*	
Ac-	C I A R L " " "	cJun(g)
Ac-	R C A R L " " "	cJun(a)
Ac-	R I A R C " " "	cJun(d)
	cFOS(161-195)	
Ac-	L T D T L Q A E T D Q L E D K K S A L Q T E I A N L L K E K E K L E F *NH2*	
Ac-	C T D T L " " "	cFos(g)
Ac-	L C D T L " " "	cFos(a)
Ac-	L T D T C " " "	cFos(d)
	gp41(555-590)	
Ac-	L L R A I E A Q Q H L L Q L T V W G I K Q L Q A R I L A V E R Y L K D Q *NH2*	
Ac-	C " " "	gp41(g)
Ac-	L C " " "	gp41(a)
Ac-	L L R A C " " "	gp41(d)

to ref. [16a]): Ac-[Cys^{555}]-gp41(555–590)-NH_2 (gp41(**g**)), Ac-[Cys^{556}]-gp41(555–590)-NH_2 (gp41(**a**)), and Ac-[Cys^{559}]-gp41(555–590)-NH_2 (gp41(**d**)). Disulfide crosslinking was performed in a manner similar to that described for the GCN4, cJun, and cFos peptide fragments. Fragment gp41(**g**) formed a covalent dimer very fast ($t_{1/2}$ ca. 22 h, Fig. 5a). The covalent dimer of gp41(**a**) was formed with $t_{1/2}$ approximately 73 h (Fig. 5b), and the dimer of gp41(**d**) was formed with $t_{1/2} < 73$ h (Fig. 5c). Among the binary mixtures of the different gp41 peptides, gp41(**g**)+gp41(**d**) produced a covalent heterodimer [gp41(**g**)+gp41(**d**)], Figure 5d. This result, along with the observed fast formation of [gp41(**g**)+gp41(**g**)] and slow formation of [gp41(**a**)+gp41(**a**)], suggests that the gp41 protein dimerizes in accord with the putative **gd** model (Fig. 1b).

Discussion

We utilized the established principles of the design of cysteine-substituted peptides to probe the recognition preferences among the cJun, cFos, GCN4 and gp41 peptides. We elected to substitute positions **a**, **d**, **g** in the N-terminal rather than in an internal part of these peptides. This follows the finding of Hodges et al., which provided strong evidence that N-terminally rather than internally linked dimers of a designer coiled-coil peptide possessed the least perturbed or the most ordered coiled-coil conformation.[20] While under strongly oxidative ($K_3Fe(CN)_6$) conditions disulfides form very fast (minutes), the mild oxidative conditions used in the trapping experiments described here resulted in extremely slow oxidation, similar to conditions employed in other studies.[19, 20] Although the disulfide formation is oxidative in nature, this process can be reversed because of the presence of unreacted thiols, thus providing near-equilibrium conditions. This applies in particular to binary mixtures of cysteine mutants of cJun, cFos, GCN4 and gp41. Heterodimer XY, if more thermodynamically stable than the initially (kinetically) trapped homodimer X_2, can form by HY-mediated reduction of X_2 to monomeric XH. There is a precedent for the use of disul-

0947-6539/96/0204-0406 $ 15.00+.25/0 Chem. Eur. J. 1996, 2, No. 4

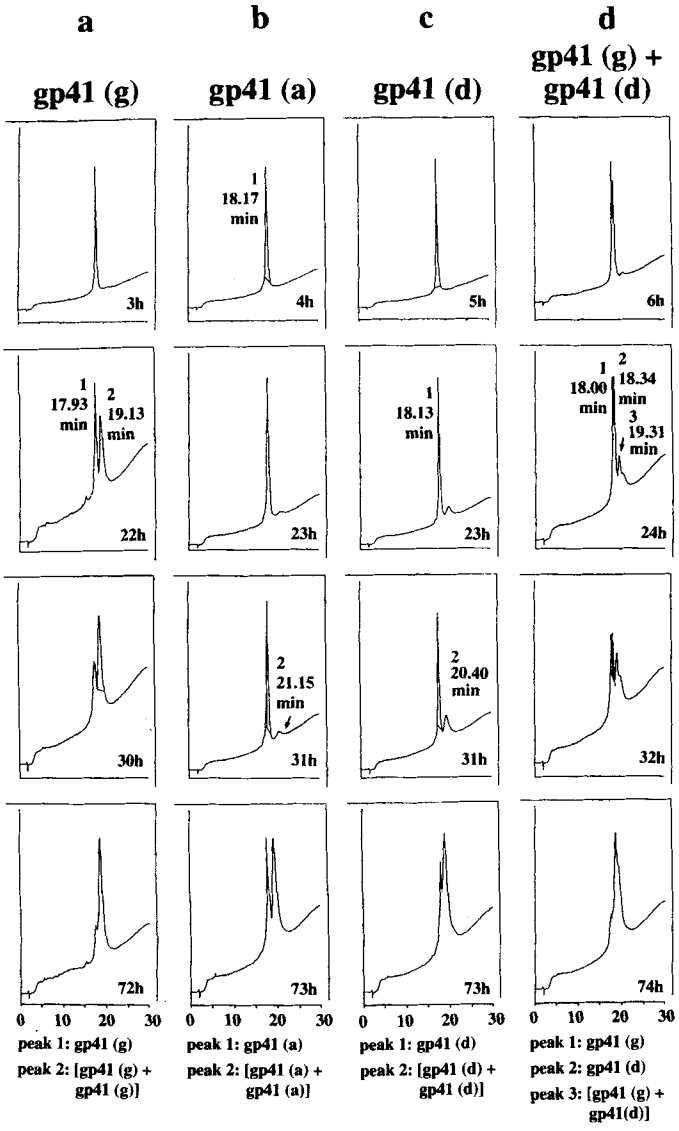

Fig. 5. HPLC traces (conditions II) of Ac-gp41(555–590)-NH_2. a) Cys^{555} (position g); b) Cys^{556} (position a); c) Cys^{559} (position **d**); d) binary mixture of Ac-[Cys^{555}]-gp41(555–590)-NH_2 and Ac-[Cys^{559}]-gp41(555–590)-NH_2.

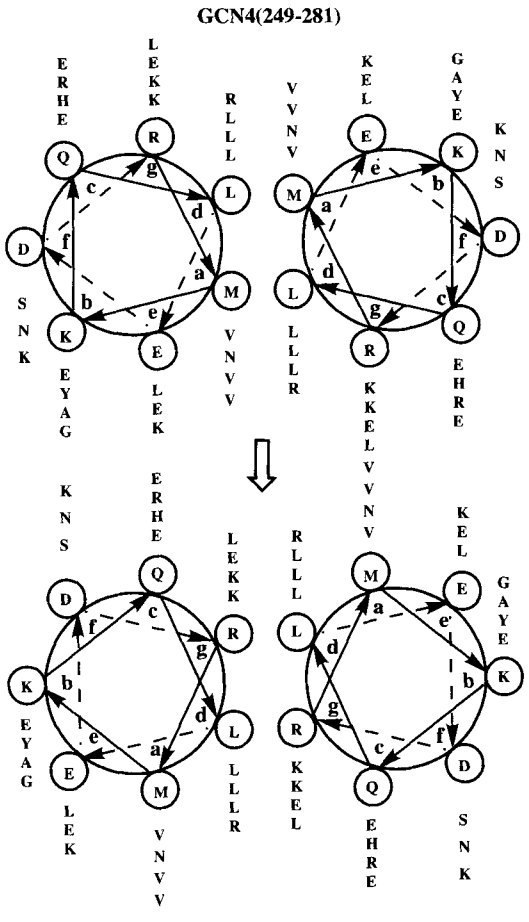

Fig. 6. **ad** (top) and corresponding **gd** (bottom) helical wheel models of GCN4(249–281) dimer.

fide trapping to determine tertiary structure, for example of *E. coli* transmembrane receptor, by measurements of iodine- or Cu^{II}(phenanthroline)$_3$-induced cross-linking rates.[21] Although macromolecular association of coiled coils is very fast, peptides described here required days to form covalent dimers, perhaps reflecting slow oxidative conditions coupled with conversion equilibria. The conditions applied provided ample time for the interacting helices to assemble in a thermodynamically preferred fashion; consequently compounds isolated and characterized from HPLC traces reflect the thermodynamically stable coiled-coil dimers.

Our crosslinking results for GCN4, cFos, and cJun are well supported by independent data obtained for intact proteins. While GCN4 forms homodimers, cFos and cJun do not (at or above room temperature), though they do form heterodimers. At the time we initiated these studies the mode of GCN4 dimerization was not known. Subsequently, X-ray structures of GCN4 dimer, free and complexed to DNA, were published.[22] Both helices in the X-ray structures appear to interact through their **ad** faces; this is in excellent agreement with our results.

The helical wheel representations of Figures 6–10 help to explain the results of our experiments. First, Figure 6 explains why GCN4 dimerized according to the **ad** and not the **gd** model. In the top (**ad**) orientation, there is knob-into-hole packing between mostly leucines (**d**) and valines (**a**), in addition to secondary stabilization by the salt-bridge formation between pairs of acidic/basic amino acids on positions **g** and **e**. The bottom (**gd**) orientation was suggested as the more stable one on the basis of theoretical computations.[15] Our results definitely exclude that orientation in an aqueous medium. The intuitive reasons for the **ad** preference are the repulsive forces between identically charged amino acids on both positions **g** as well as lack of secondary stabilizing forces between **c** (mostly acidic) and **a** (mostly hydrophobic) side chains in the **gd** model.

Figure 7 explains the inability of cJun to dimerize efficiently. First and foremost, auxiliary interactions between the helices are lacking. Position **g** features two basic amino acids, while the opposite position **e** also contains two basic and only one acidic residue, resulting in overall repulsion. In this model the specificity of interaction in leucine zippers comes from facial positions **g**, **d**, **a**, and **e**, which determine whether a particular helical protein will dimerize or not. Early views suggested that the leucine zipper dimerization was mostly mediated by hydrophobic interactions; recent findings, supported by our results, indicate that ionic forces also mediate such specificity and pairing.[23]

Figure 8 offers several reasons for low propensity of cFos to dimerize. The primary positions **a** each contain two basic amino acids, which repel each other. The secondary positions **g** (three acidic amino acids) and **e** (two acidic amino acids) also repel

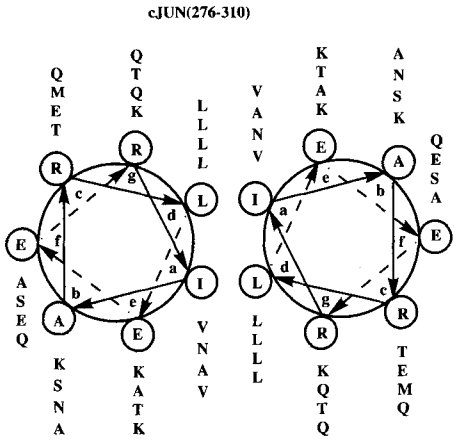

Fig. 7. An **ad** helical wheel representation of the dimer of cJun(276–310).

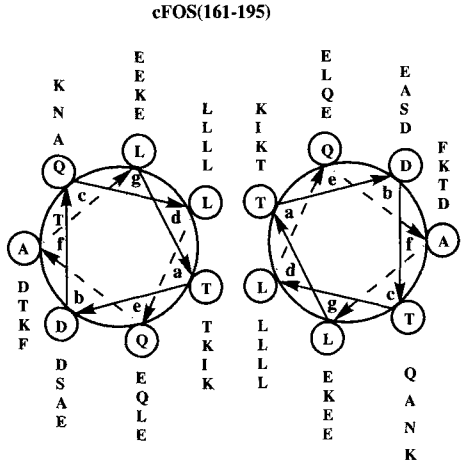

Fig. 8. An **ad** helical wheel representation of the dimer of cFos(161–195).

each other and thus destabilize the dimer. In contrast, the [cJun+cFos] dimer is greatly stabilized by the corresponding secondary positions: **g** of cJun contains two basic amino acids that are attracted to the two acidic residues on position **e** of cFos, while position **e** of cJun contains two basic amino acids that are attracted to the three acidic residues on position **g** of cFos (Fig. 9).

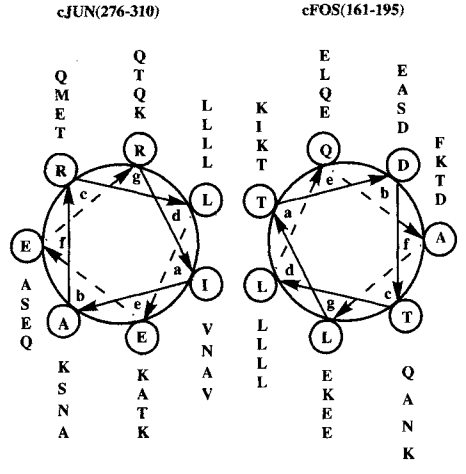

Fig. 9. An **ad** helical wheel representation of the heterodimer of cJun(276–310) and cFos(161–195).

Having validated our trapping approach on cJun, cFos and GCN4 peptides we extended our technique to gp41, which mediates HIV-1 cellular fusion, and fragments of which possess strong antiviral properties. By analogous arguments, in the **ad** model (Fig. 10, top), the primary **a** positions repel owing to the presence of glutamic acids. In addition, the secondary position

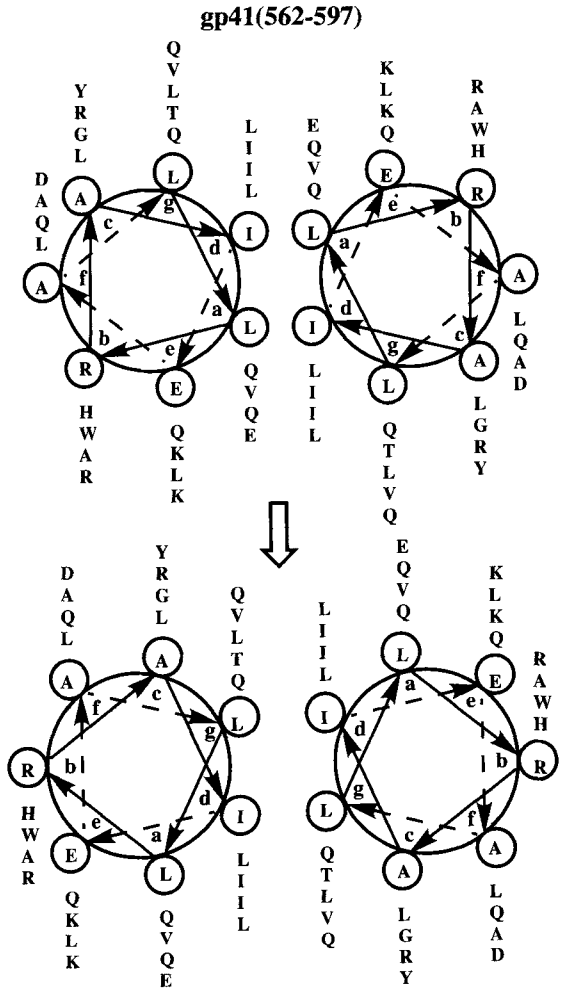

Fig. 10. **ad** (top) and corresponding **gd** (bottom) helical wheel models of gp41(562–597) dimer.

e contains an array of both acidic and basic amino acids, which have no stabilizing counterpart in the corresponding position **g**. In contrast, model **gd** (Fig. 10, bottom), obtained by simultaneous clockwise rotation of both helical wheels around their axes, features much improved interactions. The amino acids that constitute the primary contacts are all noncharged, while the secondary sphere of interactions includes arginine (position **c**), which pairs with the glutamic acid (position **a**). In summary, these qualitative arguments explain our disulfide trapping-based observations concerning the relative helical orientation preference in gp41 of HIV-1.

Finally, we attempted to use the generated information about the preferred dimerization mode of gp41 to design a simplified coiled-coil gp41 peptide possessing the full biological activity of native gp41. According to the **gd** dimerization mode of gp41 (Fig. 10, bottom), positions **f**, **b**, and **e** play only a structural role in maintaining the α-helical framework, but are not involved in intermolecular interactions within the dimer. Consequently, the

0947-6539/96/0204-0408 $ 15.00+.25/0 Chem. Eur. J. 1996, 2, No. 4

current amino acids on these positions could be substituted by alanines, possibly without any effect on the ability of these alanine-rich peptides to form α-helical dimers. A simple and reliable way to discover whether this is indeed true is to measure the biological properties of the alanine-rich peptides and compare them with the biological activities of the native peptides. The alanine-enriched (in position **f**, **b**, and **e**) peptide, Ac-[Ala(565,568,569,572,575,576,582,586,589,590)]-gp41(553–590)-NH_2, had an IC_{50} of about 30 μM against HIV-1 in MT4 cells. This compares favorably with the native gp41 fragment gp41(553–590)-NH_2, which had an IC_{50} of 2.7 μM in the same assay. This result strongly suggests that positions **f**, **b**, and **e** do not participate in either primary or secondary interactions in the gp41 coiled coil and that their major role is to support the helical propensity of gp41.

Circular dichroism (CD) studies: We further characterized the solution conformation of the monomeric and dimeric peptides under a variety of buffer conditions. First, we determined for the example of covalent dimers [GCN4(**a**)+GCN4(**a**)] (Fig. 11) and [gp41(**g**)+gp41(**g**)] (Fig. 12) whether only one stable form (i.e., monomer vs. dimer) was present within the concentration range used for the disulfide trapping. The fluorescence intensity of the dimer [GCN4(**a**)+GCN4(**a**)] increased linearly within the range of the CD experiments (5–7 μM) as a function of concentration from 0.2 to 20 μM in PBS. The fluorescence intensity of the dimer [gp41(**g**)+gp41(**g**)] also increased nearly linearly—although there could be some quenching of the fluorescence as the concentration increases. The apparent linearity of both plots suggests that one form, the dimer, prevails in solution. The ratio of $[\theta]_{222}/[\theta]_{208}$ can be utilized to distinguish between the monomeric α-helices and dimeric coiled coils. An idealized value of $[\theta]_{222}/[\theta]_{208} = 1.03$ was found for coiled-coil conformation in aqueous buffers,[24] while $[\theta]_{222}/[\theta]_{208} = 0.86$ for the single-stranded α-helix polypeptides.[24b, 25, 26]

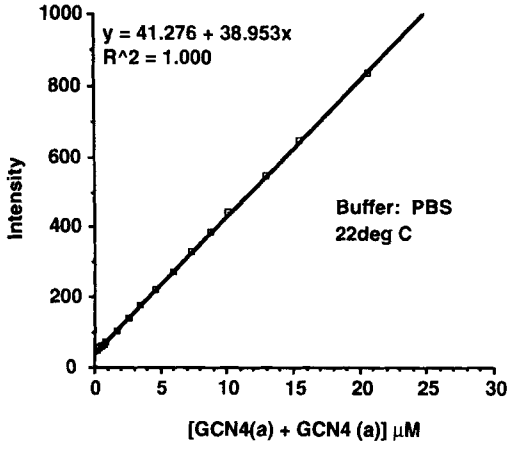

Fig. 11. Fluorescence intensity as a function of concentration for the covalent dimer of GCN4(**a**). The fluorescence intensity of Tyr was monitored by excitation at 275 nm and measurement of the emission intensity at 305 nm, PBS buffer, 22 °C.

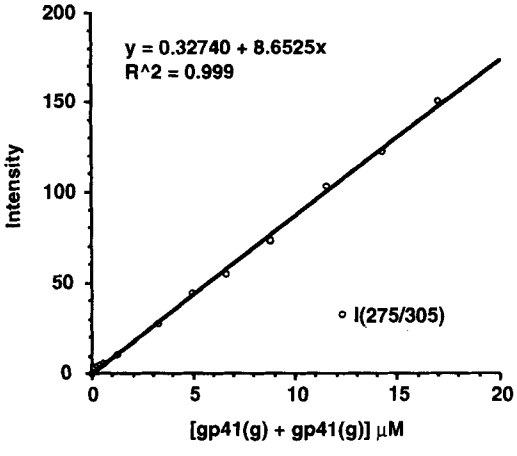

Fig. 12. Tyrosine fluorescence intensity as a function of concentration for the covalent dimer of gp41(**g**). The fluorescence intensity of Tyr was monitored by excitation at 275 nm and measurement of the emission intensity at 305 nm.

In the light of the above, Figure 13 provides evidence that cFos(**g**), GCN4(**g**) (in 30% 2,2,2-trifluoroethanol (TFE)) are monomeric, while GCN4(**g**), GCN4(**a**) and gp41(**g**) are (non-covalent) coiled coils. Addition of TFE to GCN4(**g**) dissociates the dimer to monomer, as found for other proteins.[24b, 25, 26]

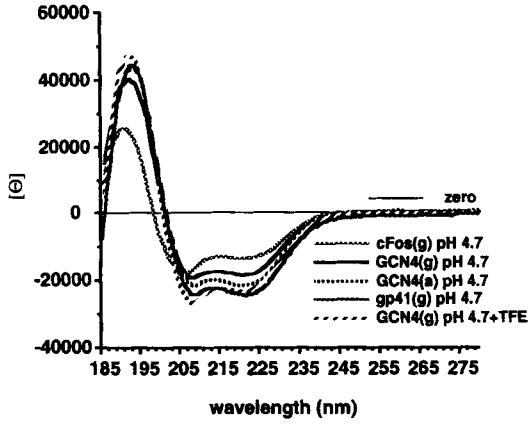

Fig. 13. CD of monomeric cFos(**g**), GCN4(**g**), GCN4(**a**), gp41(**g**) in a 50 mM phosphate buffer, pH = 4.7, and GCN4(**g**) in 50 mM phosphate buffer, pH = 4.7/30% trifluoroethanol. Concentrations used 5–7 μM.

Figure 13 also demonstrates the helical character of cysteine-substituted Fos, GCN4 and gp41. The normalized intensity for 100% α-helical content at 222 nm is $-37400\,^{\circ}cm^2\,dmol^{-1}$.[27] Thus, the percentage α-helicity is 37.5 for cFos(**g**), 47.6 for GCN4(**g**), 58.3 for GCN4(**a**), 66.5 for gp41(**g**) and 62.6 for GCN4(**g**) in 30% TFE. In addition, "mutant" peptides incorporating cysteine at different positions maintain their high α-helicity.

As a positive control, the CD spectra of covalent dimers (Fig. 14) all show similar intensities at 222 and 208 nm, consis-

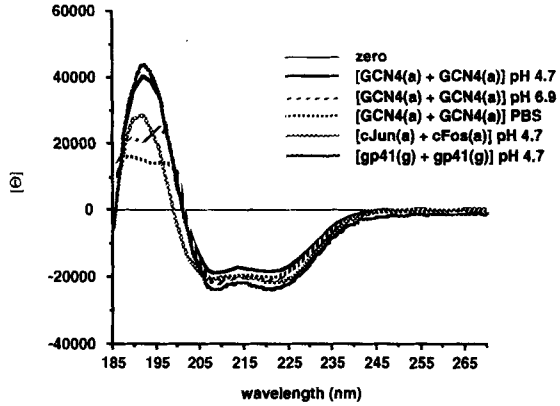

Fig. 14. CD of covalent dimers of GCN4(**a**) and gp41(**g**) and of heterodimer [cJun(**a**)+cFos(**a**)], all at pH = 4.7 (50 mM phosphate buffer) as well as of covalent dimers of GCN4(**a**) in PBS and in 50 mM phosphate buffer, pH = 6.9. Concentrations used 5–7 μM.

tent with a dimeric zipper structure with α-helicities ranging between 65.0–47.9%. Thus, neither pH (4.7 vs. 6.9, both 50 mM phosphate buffer) nor the ionic strength (50 mM phosphate buffer vs. 150 mM PBS, both pH = 6.9) greatly influences the α-helicity of [GCN4(**a**)+GCN4(**a**)]. We also demonstrate that heterodimeric [cJun(**a**)+cFos(**a**)] and the covalent dimer of [gp41(**g**)+gp41(**g**)] are highly helical, 58.7% and 65.0%, respectively (Fig. 14).

Similarly to the covalent dimer of GCN4, [GCN4(**a**)+GCN4(**a**)], [gp41(**g**)+gp41(**g**)] is not very sensitive to environmental changes such as pH (64.5% helicity at 4.7 and 50.0% at 6.9) or ionic strength (50.0% in PBS vs. 47.6% in 50 mM phosphate buffer, both pH = 4.7).

Conclusions

The significance of our results, we believe, is twofold.

First, we postulate that the cross-linking experiments described above can provide detailed structural information and distinguish between several possible models. We verified our technique by confirming the known properties of the transcription factors GCN4, cJun, and cFos. We confirmed independently that GCN4 dimerizes in solution through its **ad** rather than **gd** interface (as suggested by molecular dynamics[15]), as it does in the solid state. We also demonstrated that the **ad** type of interaction is dominant for cJun–cFos heterodimers, while gp41 of HIV-1 dimerizes in the **gd** fashion. This kind of information can be utilized in the design of molecules able to interfere with coiled-coil-mediated macromolecular dimerization.

Secondly, our approach, unlike X-ray or NMR structure determination, permits evaluation of the tertiary structure under a variety of experimental conditions, such as pH, solvent, temperature, presence of lipid phase, etc. Many of the coiled-coil proteins may present a different mutual orientation when they are membrane-bound. This could happen because the membrane might engage the hydrophobic amino acids (position **a**) while dehydrating the hydrophilic amino acids (position **g**) and forcing them to create salt bridges, thus facilitating **gd** face recognition, as depicted in Figure 6 (bottom). At present we are further exploiting this technique to gather structural information about proteins of medicinal interest under near-physiological conditions.

During or after our work was completed, several X-ray structures pertinent to our studies were published, namely those of cFos–cJun bound to DNA[28] and of GCN4.[22, 29] All the structures show a good agreement with regard to the global fold of the leucine zipper proteins. Both GCN4 homodimer and Jun–Fos heterodimer in the solid state utilize their **ad** faces, which, again, is in complete agreement with our solution results from disulfide trapping as a structural tool. While the **ad**-type interaction is often thought to be favored in leucine-zipper dimer, no direct structural evidence of it existed for the Jun–Fos dimer at the time our work was completed. In fact, computations for the dimer of GCN4 suggested that the **gd** dimer is more stable than the **ad** dimer.[15] Our results obtained in solution and in the solid state[28] provide the first (and consistent) experimental details about the nature of Jun–Fos dimerization.

Experimental Section

Peptide synthesis: All the peptides were synthesized on a 0.1 mM scale with Rink amide resin. We utilized 9-fluorenylmethoxycarbonyl (Fmoc)/*t*Bu chemistry on a 431 ABI synthesizer in accordance with in-house synthetic protocols. Briefly, the peptides were assembled by stepwise addition of Fmoc/*t*Bu amino acids (10 equiv), the coupling was mediated by benzotriazol-1-yl-*N*-tetramethyluronium hexafluorophosphate (HBTU), and Fmoc-deprotection was effected by piperidine/*N*-methylpyrrolidone (NMP) solution. The N-terminal amino group was then acetylated (when indicated in the formula) by 1 M acetic anhydride/NMP/1-hydroxybenzotriazole (HOBt), and the peptide resin was washed and dried in vacuo. The peptides were deprotected and cleaved from the resin with thioanisole/dithioethane/anisole/trifluoroacetic acid (TFA) 5:3:2:90 (v/v) (50 mL) for 3 h, after which the resin was filtered off, cold ethyl ether (200 mL) added to the filtrate, and the resulting white precipitate isolated and dried in vacuo. The crude peptides were purified to homogeneity on C_{18} reverse-phase HPLC with a 0.1% TFA/acetonitrile (B) and 0.1% TFA/water (A) binary gradient. All the pure peptides gave correct amino acid analyses and molecular masses (FAB-MS or ion spray). The HPLC traces in Figures 2–4 were generated under conditions I: Waters C_{18} reverse-phase column RCM 8 × 10, flow 2.5 mL min^{-1}, monitored at 220 nm, gradient 10–60% B over 10 min, followed by 60–90% B over 3 min and 90–10% B over 2 min. The HPLC traces in Figure 5 were generated under conditions II: Vydac 218 TP 54 C_{18} RP column, 0–67% B over 30 min, monitored at 220 nm, flow 1.5 mL min^{-1}.

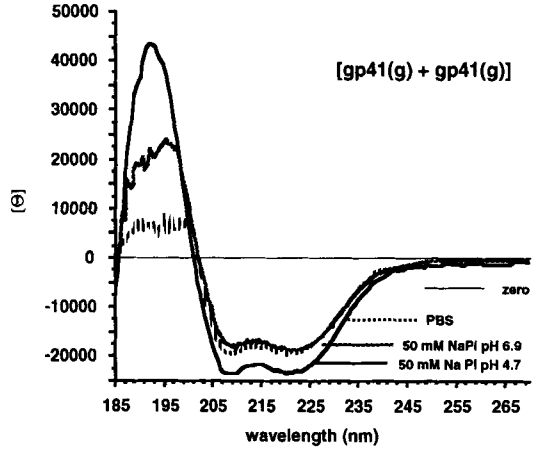

Fig. 15. CD of covalent dimer of gp41(**g**) in PBS, and at pH = 4.7 and pH = 6.9, both in 50 mM phosphate buffer. Concentrations used 5–7 μM.

Disulfide trapping experiments: A stock solution of each peptide was prepared and an appropriate amount transferred to the final volume of 1 mL 50 mM sodium phosphate buffer (pH = 4.7), resulting in 5 μM L^{-1} concentration of each peptide. The disulfide bonds were then allowed to form spontaneously by use of buffer-dissolved oxygen in septum-equipped vials. Under the experimental conditions the ratio of oxygen to thiol was about 250, and thus oxygen is not the rate-limiting component. The disulfide formation rates were monitored over time by RP-HPLC with a C_{18} stationary phase. HPLC fractions were analyzed by FAB-MS and amino-acid analysis, resulting in full and unambiguous characterization of all components. The pH of 4.7 was chosen as a compromise between solubilities of the investigated compounds; indeed Figure 15 demonstrates that the α-helical content of gp41(g) dimer is only slightly higher at pH = 4.7 (64.5%) than at pH 6.9 (53.0%).

CD measurements: CD spectra were obtained with a Jasco J-720 spectropolarimeter over the wavelength range 280 to 185 nm with a step resolution of 0.5 nm at 50 nm min^{-1} in a 0.5-cm cell at room temperature (22 °C). Eight scans were added together per spectrum, and a baseline spectrum was subtracted for each sample. Results are expressed in terms of mean residue ellipticity [θ] in units of °cm^2 dmol^{-1}. The helical contents were calculated by literature methods [27]. Sample preparation: 0.02 mg of each peptide was dissolved in 1 mL of buffer (indicated in figure legends). The concentrations obtained were in the range of 5–7 μM L^{-1} and were experimentally confirmed (within 5% deviation) by UV-determined peptide concentrations.

Abbreviations: M_c: molecular mass calculated from isotopic values; M_f: molecular mass found. Since ^{13}C is about 1.1% abundant, the molecular mass observed will be larger than that calculated on the basis of isotopic values; there is an increment of about 1 dalton per 100 carbon atoms. On average, the difference will be ca. 1.5–2 daltons for the monomers and ca. 3–4 daltons for the dimers.

Ac-[Cys^{249}]-GCN4(249–281)-NH_2 (GCN4(**g**)): M_c = 3982.12, M_f = 3983.4; Asx 2.97 (3), Ser 0.83 (1), Glx 7.01 (7), Gly 0.95 (1), Ala 1.00 (1), Val 2.79 (3), Met 0.99 (1), Leu 6.03 (6), Tyr 0.94 (1), His 0.88 (1), Lys 4.60 (5), Arg 1.98 (2), Cys 0.83 (1).

Ac-[Cys^{250}]-GCN4(249–281)-NH_2 (GCN4(**a**)): M_c = 4007.18, M_f = 4008.8; Asx 3.18 (3), Ser 0.90 (1), Glx 7.12 (7), Gly 1.06 (1), Ala 1.10 (1), Val 3.05 (3), Leu 6.03 (6), Tyr 0.94 (1), His 0.88 (1), Lys 4.81 (5), Arg 3.13 (3), Cys 0.89 (1).

0947-6539/96/0204-0410 $ 15.00+.25/0 Chem. Eur. J. 1996, 2, No. 4

Ac-[Cys^{253}]-GCN4(249–281)-NH_2 (GCN4(**d**)): M_c = 4025.13, M_f = 4026; Asx 3.08 (3), Ser 0.86 (1), Glx 7.29 (7), Gly 1.01 (1), Ala 1.05 (1), Val 2.89 (3), Met 0.98 (1), Leu 5.27 (5), Tyr 0.96 (1), His 0.85 (1), Lys 4.70 (5), Arg 3.07 (3), Cys 0.83 (1).

Ac-[Cys^{276}]-cJun(276–310)-NH_2 (cJun(**g**)): M_c = 3927.10, M_f = 3927.6; Asx 2.04 (2), Thr 3.01 (3), Ser 1.96 (2), Glx 8.08 (8), Ala 5.28 (5), Val 2.05 (2), Met 0.99 (1), Ile 0.94 (1), Leu 5.15 (5), Lys 3.72 (4), Arg 0.98 (1), Cys 0.79 (1).

Ac-[Cys^{277}]-cJun(276–310)-NH_2 (cJun(**a**)): M_c = 3970.12, M_f = 3970.9; Asx 2.03 (2), Thr 2.99 (3), Ser 1.76 (2), Glx 8.28 (8), Ala 5.41 (5), Val 1.89 (2), Met 1.07 (1), Leu 5.04 (5), Lys 3.65 (4), Arg 1.87 (2), Cys 0.75 (1).

Ac-[Cys^{280}]-cJun(276–310)-NH_2: cJun(**d**) M_c = 3970.11, M_f = 3971.7; Asx 1.90 (2), Thr 2.87 (3), Ser 1.69 (2), Glx 7.78 (8), Ala 5.21 (5), Val 1.85 (2), Met 1.01 (1), Ile 0.78 (1), Leu 3.94 (4), Lys 3.36 (4), Arg 1.61 (2), Cys 0.80 (1).

Ac-[Cys^{161}]-cFos(161–195)-NH_2 (cFos(**g**)): M_c = 4063.08, M_f = 4064.4; Asx 3.94 (4), Thr 3.67 (4), Ser 0.86 (1), Glx 9.06 (9), Ala 3.05 (3), Ile 1.00 (1), Leu 6.03 (6), Phe 1.02 (1), Lys 4.61 (5), Cys 0.82 (1).

Ac-[Cys^{162}]-cFos(161–195)-NH_2 (cFos(**a**)): M_c = 4075.11, M_f = 4076.4; Asx 4.06 (4), Thr 2.89 (3), Ser 0.89 (1), Glx 9.27 (9), Ala 3.10 (3), Ile 1.05 (1), Leu 7.16 (7), Phe 1.04 (1), Lys 4.68 (5), Cys 0.86 (1).

Ac-[Cys^{165}]-cFos(161–195)-NH_2 (cFos(**d**)): M_c = 4063.08, M_f = 4063.2; Asx 4.05 (4), Thr 3.72 (4), Ser 0.92 (1), Glx 9.33 (9), Gly 1.15 (1), Ala 3.03 (3), Ile 1.08 (1), Leu 6.24 (6), Phe 1.04 (1), Lys 4.78 (5), Cys 0.85 (1).

Ac-[Cys^{555}]-gp41(555–590)-NH_2 (gp41(**g**)): M_c = 4285.41, M_f = 4287; Asx 1.39 (1), Thr 0.87 (1), Glx 8.24 (8), Gly 1.37 (1), Ala 3.88 (4), Val 2.05 (2), Ile 2.47 (3), Leu 6.74 (7), Tyr 1.04 (1), His 1.22 (1), Lys 1.90 (2), Arg 2.81 (3), Trp 0.79 (1), Cys 0.76 (1).

Ac-[Cys^{556}]-gp41(555–590)-NH_2 (gp41(**a**)): M_c = 4285.41, M_f = 4287; Asx 1.18 (1), Thr 1.00 (1), Glx 8.18 (8), Gly 1.39 (1), Ala 3.92 (4), Val 2.03 (2), Ile 2.47 (3), Leu 6.66 (7), Tyr 1.03 (1), His 0.97 (1), Lys 1.90 (2), Arg 2.72 (3), Trp 0.66 (1), Cys 0.86 (1).

Ac-[Cys^{559}]-gp41(555–590)-NH_2 (gp41(**d**)): M_c = 4285.41, M_f = 4287; Asx 1.35 (1), Thr 0.88 (1), Glx 8.38 (8), Gly 1.02 (1), Ala 3.91 (4), Val 2.13 (2), Ile 1.64 (2), Leu 7.62 (8), Tyr 1.11 (1), His 0.98 (1), Lys 1.84 (2), Arg 2.78 (3), Trp 0.75 (1), Cys 1.14 (1).

Disulfide trapping experiments:

Figure 2a, peak 1, [GCN4(**g**)+GCN4(**g**)]: M_c = 7962.2, M_f = 7965.9.

Figure 2b, peak 1, [GCN4(**a**)+GCN4(**a**)]: M_c = 8012.4, M_f = 8016.2.

Figure 2c, peak 1, [GCN4(**d**)+GCN4(**d**)]: M_c = 8048.3, M_f = 8052.2.

Figure 4a, peak 1, [cJun(**g**)+cFos(**g**)]: M_c = 7988.2, M_f = 7992; Asx 6.14 (6), Thr 6.96 (7), Ser 3.03 (3), Glx 17.44 (17), Ala 8.34 (8), Val 1.82 (2), Met 0.95 (1), Ile 1.77 (2), Leu 10.65 (11), Phe 0.93 (1), Lys 9.03 (9), Arg 0.94 (1).

Figure 4b, peak 1, [cJun(**a**)+cFos(**a**)]: M_c = 8043.2, M_f = 8047; Asx 6.26 (6), Thr 5.78 (6), Ser 2.70 (3), Glx 17.16 (17), Ala 8.39 (8), Val 1.99 (2), Met 1.00 (1), Ile 0.98 (1), Leu 12.12 (12), Phe 0.98 (1), Lys 8.69 (9), Arg 1.94 (2).

Figure 4c, peak 1, [cJun(**d**)+cFos(**d**)]: M_c = 8031.18, M_f = 8035; Asx 6.21 (6), Thr 6.81 (7), Ser 2.71 (3), Glx 17.43 (17), Ala 8.27 (8), Val 2.00 (2), Met 0.95 (1), Ile 1.90 (2), Leu 10.18 (10), Phe 0.94 (1), Lys 8.84 (9), Arg 1.77 (2).

[cFos(**d**)+GCN4(**d**)]: M_c = 8086.2, M_f = 8090; Asx 6.96 (7), Thr 3.73 (4), Ser 2.01 (2), Glx 15.96 (16), Gly 1.08 (1), Ala 3.83 (4), Val 3.39 (3), Met 0.84 (1), Ile 1.32 (1), Leu 10.95 (11), Tyr 0.90 (1), Phe 0.94 (1), His 1.13 (1), Lys 9.81 (10), Arg 3.15 (3).

[GCN4(**g**)+GCN4(**a**)]: M_c = 7987.3, M_f = 7992; Asx 6.05 (6), Ser 1.85 (2), Glx 14.18 (14), Gly 2.16 (2), Ala 2.09 (2), Val 5.78 (6), Met 0.88 (1), Leu 11.94 (12), Tyr 1.94 (2), His 2.15 (2), Lys 10.25 (10), Arg 4.74 (5).

Figure 5a, peak 2, [gp41(**g**)+gp41(**g**)]: M_c = 8568.8, M_f = 8571.2; Asx 2.21 (2), Thr 1.75 (2), Glx 16.44 (16), Gly 2.40 (2), Ala 7.74 (8), Val 3.94 (4), Ile 6.45 (6), Leu 14.02 (14), Tyr 1.77 (2), His 1.94 (2), Lys 3.72 (4), Arg 5.65 (6).

Figure 5b, peak 2, [gp41(**a**)+gp41(**a**)]: M_c = 8568.8, M_f = 8571.5; Asx 2.25 (2), Thr 1.73 (2), Glx 16.35 (16), Gly 2.49 (2), Ala 7.85 (8), Val 3.90 (4), Ile 5.72 (6), Leu 14.07 (14), Tyr 1.98 (2), His 1.97 (2), Lys 3.82 (4), Arg 5.86 (6).

Figure 5d, peak 3, [gp41(**g**)+gp41(**d**)]: M_c = 8568.8, M_f = 8571.5; Asx 2.50 (2), Thr 1.83 (2), Glx 16.37 (16), Gly 2.32 (2), Ala 7.70 (8), Val 4.06 (4), Ile 4.76 (5), Leu 14.73 (15), Tyr 1.75 (2), His 1.72 (2), Lys 3.86 (4), Arg 6.34 (6).

Acknowledgments: We thank B. Chestnut for the amino-acid analyses and capillary electrophoresis used in verifying the purity of our compounds (data not shown) as well as L. St. John for the mass spectrometry data. The continued support of Drs. R. W. Morrison and Tom Krenitsky is gratefully acknowledged.

Received: January 26, 1995
Revised version: October 6, 1995 [F70]

[1] a) M. Noguchi, Y. Nakamura, S. M. Russell, S. F. Ziegler, M. Tsang, X. Cao, W. J. Leonard, *Science* **1993**, *262*, 1877–1880; b) S. M. Russel, A. D. Keegan, N. Harada, Y. Nakamura, M. Noguchi, P. Leland, M. C. Friedmann, A. Miyajima, R. K. Puri, W. E. Paul, W. J. Leonard, *ibid.* **1993**, *262*, 1880–1883; c) M. Kondo, T. Takeshita, N. Ishii, M. Nakamura, S. Watanabe, K. Arai, K. Sugamura, *ibid.* **1993**, *262*, 1874–1877.

[2] A. M. De Vos, M. Ultsch, A. Kossiakoff, *Science* **1992**, *255*, 306–312.

[3] Review: P. Sheterline, *Protein Profile* **1994**, *1*, 123–168.

[4] T.-H. Lin, D. P. Grandgenett, *Protein Eng.* **1991**, *4*, 435–441.

[5] A. Jacobo-Molina, J. Ding, R. G. Nanni, A. D. Clark, Jr., X. Lu, C. Tantillo, R. L. Williams, G. Kamer, A. L. Ferris, P. Clark, A. Hizi, S. H. Hughes, E. Arnold, *Proc. Natl. Acad. Sci. USA* **1993**, *90*, 6320–6324.

[6] L. A. Zwelling, W. M. Perry, *Mol. Endocrinol.* **1989**, *3*, 603–604.

[7] a) B. M. Dutia, M. C. Frame, J. H. Subak-Sharpe, W. N. Clark, H. S. Marsden, *Nature* **1986**, *321*, 439–441; b) T. D. Chung, J. Luo, J. P. Wymer, C. C. Smith, L. Aurelian, *J. Gen. Virol.* **1991**, *72*, 1139–1144.

[8] E. Flemington, S. H. Speck, *Proc. Natl. Acad. Sci. USA* **1993**, *87*, 9459–9463.

[9] W. J. Koch, J. Inglese, W. C. Stone, R. J. Lefkowitz, *J. Biol. Chem.* **1993**, *268*, 8256–8260.

[10] a) R. W. Doms, P. L. Earl, S. Chakrabarti, B. Moss, *J. Virol.* **1990**, *64*, 3537–3540; b) D. J. Thomas, J. S. Wall, J. F. Hainfeld, M. Kaczorek, F. P. Booy, B. L. Trus, F. A. Eiserling, A. C. Steven, *ibid.* **1991**, *65*, 3797–3803; c) M. Schawaller, G. E. Smith, J. J. Skehel, D. C. Wiley, *Virology* **1989**, *172*, 367–369.

[11] C. Wild, T. Oas, C. McDanal, D. Bolognesi, T. Matthews, *Proc. Natl. Acad. Sci. USA* **1992**, *89*, 10537–10541.

[12] D. Frechet, J. D. Guitton, F. Herman, D. Faucher, G. Helynck, B. Monegier du Sorbier, J. P. Ridoux, E. James-Surcouf, M. Vuilhorgne, *Biochemistry* **1994**, *33*, 42–50.

[13] W. H. Landschulz, P. F. Johnson, S. L. McKnight, *Science* **1988**, *240*, 1759–1764.

[14] J. C. Hu, E. K. O'Shea, P. S. Kim, R. T. Sauer, *Science* **1990**, *250*, 1400–1403.

[15] A. Tropsha, J. P. Bowen, F. K. Brown, J. S. Kizer, *Proc. Natl. Acad. Sci. USA* **1991**, *88*, 9488–9492.

[16] a) J. Cao, L. Bergeron, E. Helseth, M. Thali, H. Repke, J. Sodroski, *J. Virol.* **1993**, *67*, 2747–2755; b) J. W. Dubay, S. J. Roberts, B. Brody, E. Hunter, *ibid.* **1992**, *66*, 4748–4756.

[17] a) J. P. Doucet, S. P. Squinto, N. G. Bazan in *Molecular Neurobiology* (Ed.: N. G. Bazan), Humana, **1990**, 27–55; b) P. Angel, M. Karin, *Biochim. Biophys. Acta* **1991**, *1072*, 129–157.

[18] a) R. Turner, R. Tjian, *Science* **1989**, *243*, 1689–1694; b) R. Gentz, F. J. Rauscher III, C. Abate, T. Curran, *ibid.* **1989**, *243*, 1695–1699.

[19] E. K. O'Shea, R. Rutkowski, W. F. Stafford III, P. S. Kim, *Science* **1989**, *245*, 646–648.

[20] N. Zhou, C. M. Kay, R. S. Hodges, *Biochemistry* **1993**, *32*, 3178–3187.

[21] a) A. A. Pakula, M. I. Simon, *Proc. Natl. Acad. Sci. USA* **1992**, *89*, 4144–4148; b) B. A. Lynch & D. E. Koshland, Jr., *ibid.* **1991**, *88*, 10402–10406.

[22] a) E. K. O'Shea, J. D. Klemm, P. S. Kim, T. Alber, *Science* **1991**, *254*, 539–544; b) T. E. Ellenberger, C. J. Brandl, K. Struhl, S. C. Harrison, *Cell* **1992**, *71*, 1223–1237.

[23] a) O. D. Monera, C. M. Kay, R. S. Hodges, *Biochemistry* 1994, *33*, 3862–3871; b) D. G. Myszka, I. M. Chaiken, *ibid.* **1994**, *33*, 2363–2372.

[24] a) R. S. Hodges, A. K. Saund, P. C. S. Chong, S. A. St.-Pierre, R. E. Reid, *J. Biol. Chem.* **1981**, *256*, 1214–1224; b) S. Y. M. Lau, A. K. Taneja, R. S. Hodges, *ibid.* **1984**, *259*, 13253–132361; c) R. S. Hodges, P. D. Semczuk, A. K. Taneja, C. M. Kay, J. M. R. Parker, C. T. Mant, *Pept. Res.* **1988**, *1*, 19–30; d) R. S. Hodges, N. E. Zhou, C. M. Kay, P. D. Semczuk, *ibid.* **1990**, *3*, 123–137; e) N. E. Zhou, C. M. Kay, R. S. Hodges, *Biochemistry* **1992**, *31*, 5739–5746.

[25] N. E. Zhou, C. M. Kay, R. S. Hodges, *J. Biol. Chem.* **1992**, *267*, 2664–2670.

[26] M. Engel, R. W. Williams, B. W. Erickson, *Biochemistry* **1991**, *30*, 3161–3169.

[27] Y.-H. Chen, J. T. Yang, K. H. Chau, *Biochemistry* **1974**, *13*, 3350–3359.

[28] J. N. M. Glover, S. C. Harrison, *Nature* **1995**, *373*, 257–261.

[29] P. B. Harbury, T. Zhang, P. S. Kim, T. Alber, *Science* **1993**, *262*, 1401–1407.